

# The Transition State in Magnetization Reversal

G. Brown<sup>1,2</sup>, M. A. Novotny<sup>3</sup>, Per Arne Rikvold<sup>2,4</sup>

<sup>1</sup>*Center for Computational Sciences, Oak Ridge National Laboratory, Oak Ridge, TN 37831*

<sup>2</sup>*CSIT, Florida State University, Tallahassee, FL 32306*

<sup>3</sup>*Department of Physics and Astronomy and ERC, Mississippi State University, Mississippi State, MS 39762*

<sup>4</sup>*Department of Physics and MARTECH, Florida State University, Tallahassee, FL 32306*

(December 28, 2021)

We consider a magnet with uniaxial anisotropy in an external magnetic field along the anisotropy direction, but with a field magnitude smaller than the coercive field. There are three representative magnetization configurations corresponding to three extrema of the free energy. The equilibrium and metastable configurations, which are magnetized approximately parallel and antiparallel to the applied field, respectively, both correspond to local free-energy minima. The third extremum configuration is the saddle point separating these minima. It is also called the transition state for magnetization reversal. The free-energy difference between the metastable and transition-state configurations determines the thermal stability of the magnet. However, it is difficult to determine the location of the transition state in both experiments and numerical simulations. Here it is shown that the computational Projective Dynamics method, applied to the time dependence of the total magnetization, can be used to determine the transition state. From large-scale micromagnetic simulations of a simple model of magnetic nanowires with no crystalline anisotropy, the magnetization associated with the transition state is found to be linearly dependent on temperature, and the free-energy barrier is found to be dominated by the entropic contribution at reasonable temperatures and external fields. The effect of including crystalline anisotropy is also discussed. Finally, the influence of the spin precession on the transition state is determined by comparison of the micromagnetic simulations to kinetic Monte Carlo simulations of precession-free (overdamped) dynamics.

Since magnetic storage depends on the ability to quickly assign a magnetic orientation to a specific region of a medium, in which spontaneous reorientation is suppressed, understanding the process of magnetization reversal is technologically important. In magnetic fields smaller than the coercive value, the two states of the magnet important to information storage are free-energy minima separated by a free-energy barrier. The minimum corresponding to a magnetization parallel to the field is truly stable, while the minimum corresponding to the antiparallel magnetization is higher in energy and is therefore metastable. The free-energy maximum along the most likely path between the minima is a saddle point. To effectively engineer processes such as hybrid recording,<sup>1</sup> which use lower-than-coercive applied fields to assign magnetic orientations in high-coercivity magnetic materials, a thorough understanding of the magnetization reversal is needed. Properties of the free energy near the minima and saddle point often control the nonequilibrium dynamics of a system. For example, the free-energy difference between a minimum and the saddle point, the barrier height, is a measure of the stability of the magnetization associated with that minimum, while the curvature of the free energy near a minimum is a measure of the “attempt frequency” of escapes over the barrier. While the free-energy minima can be easily located as local maxima in histograms of the state of the system, the saddle point has proven much harder to measure. In this paper we present a method based on the Projective Dynamics method<sup>2,3,4</sup> for determining the saddle point in magnetization reversal of nanoscale magnets, and then investigate the free-energy barrier associated with the process.

The particular magnetic system considered in this paper is based on iron nanomagnets fabricated using STM-assisted chemical vapor deposition.<sup>5</sup> These magnetic pillars are modeled by a one-dimensional array of 17 spins along the  $z$  axis, each a unit vector  $\hat{S}_i$  representing the local orientation of the magnetization. The total energy of the pillar is given by

$$E = -\frac{J}{2} \sum_{i,j} \hat{S}_i \cdot \hat{S}_j - \frac{D}{2} \sum_{i,j \neq i} \hat{S}_i^t \mathbf{T}_{i,j} \hat{S}_j - K \sum_i (S_{i,z})^2 + B \sum_i S_{i,z} , \quad (1)$$

where  $J$  is the exchange energy,  $K$  is the uniaxial anisotropy energy,  $B$  is the strength of the external field oriented parallel to  $-\hat{z}$ ,  $D$  is the strength of the dipole-dipole interactions in energy units, and  $\mathbf{T}_{i,j} = (3\hat{z}\hat{z}^t - \mathbf{1})/|j-i|^3$  is the dimensionless dipole-dipole interaction tensor. The sum for the exchange energies is over nearest neighbors and includes a self interaction so that the exchange energy (and the associated effective field) is zero for parallel neighbors. For the 17-spin iron nanopillars, discussed previously in Ref. [6], the dimensionless energy corresponds to  $J=1.6 \times 10^{-12}$  erg,  $D=4.1 \times 10^{-12}$  erg, and  $B=1.9 \times 10^{-12}$  erg for a field of 1000 Oe. Dipole-dipole interactions along the pillar provide a strong uniaxial anisotropy, even for  $K=0$ .

For micromagnetic dynamics, each vector precesses around a local field  $\vec{H}_i = -dE/d\hat{S}_i$  according to the Landau-Lifshitz-Gilbert (LLG) equation<sup>7,8</sup>

$$\frac{d\hat{S}_i}{dt} = \frac{\gamma_0}{1 + \alpha^2} \hat{S}_i \times [\vec{H}_i - \alpha \hat{S}_i \times \vec{H}_i] , \quad (2)$$

where the scaled electron gyromagnetic ratio  $\gamma_0 = 9.26 \times 10^{21}$  Hz/erg for this system. The phenomenological damping parameter  $\alpha = 0.1$  was chosen to give underdamped dynamics.

Previously,<sup>9</sup> we have shown that the Projective Dynamics method<sup>2,3,4</sup> can be used to locate the saddle point. The computational Projective Dynamics method involves projecting the original description of the dynamics in terms of a large number of variables onto a completely stochastic description in terms of one or two variables. In this paper, Eq (1) has 34 independent variables which are projected onto a single, slowly varying variable: the  $z$ -component of the total magnetization,  $M_z$ . Furthermore, the values of  $M_z$  are binned, and the transition rates between bins are measured. For instance, the probability that  $M_z$  starts a given time interval in one bin and ends the interval in the adjacent bin corresponding to smaller values of  $M_z$  is called the “growth” probability,  $P_{\text{grow}}$ , since it corresponds to an increase in the volume of stable magnetization. The probability of moving to the opposite neighboring bin is  $P_{\text{shrink}}$ .

The measured  $P_{\text{grow}}$  and  $P_{\text{shrink}}$  for an applied field of  $H=1000$  Oe, a temperature of  $T=10$  K, and  $K=0$  are shown in the inset of Fig. 1 as the solid and broken curves, respectively. For magnetizations with  $P_{\text{grow}} > P_{\text{shrink}}$ , on average the magnetization decreases with time, while it increases, on average, for magnetizations with  $P_{\text{shrink}} > P_{\text{grow}}$ . Where  $P_{\text{grow}} = P_{\text{shrink}}$  the average rate of change is zero, and a local minimum or maximum in the free energy occurs. The right-most crossing of  $P_{\text{grow}}$  and  $P_{\text{shrink}}$  is the free-energy minimum corresponding to the metastable magnetization antiparallel to the applied field. The crossing associated with the free-energy minimum of the stable magnetization (near  $M_z = -1$ ) is not shown. The left-most crossing shown in the figure corresponds to the free-energy saddle point separating the metastable and stable wells.

The value of  $M_z$  at the saddle point for  $H=1000$  Oe and  $K=0$  is shown in Fig. 1 vs  $T$  as circles with error bars. These values were estimated from the intersection of lines fit to  $P_{\text{grow}}$  and  $P_{\text{shrink}}$  in the region near the crossing. The measurement errors were taken to be  $\pm 0.01$ , based on the size of the region where  $P_{\text{grow}} \approx P_{\text{shrink}}$ . For low  $T$ , the estimated value of  $M_z$  depends almost linearly on temperature. Good agreement exists between the estimated values and the line of best fit, which was determined from the data for  $T \leq 100$  K and is shown as the solid line in Fig. 1.

The Projective Dynamics method can also be used to estimate the free-energy barrier for the reversal process. In equilibrium, the total time spent in the  $i$ th  $M_z$  bin,  $h(i)$ , is related to the growing and shrinking probabilities by<sup>3,4</sup>

$$h(i) = [1 + P_{\text{shrink}}(i-1)h(i-1)] / P_{\text{grow}}(i), \quad h(1) = 1/P_{\text{grow}}(1) . \quad (3)$$

The time  $h(i)$  is also related to the free energy by the Boltzmann factor  $h(i) \propto \exp(-F(i)/k_B T)$ . Taking the bin containing the saddle point to be  $i_s$ , and that containing the metastable minimum to be  $i_m$ , the free-energy barrier is  $\Delta F = k_B T \ln[h(i_m)/h(i_s)]$ . The measured  $\Delta F$  for  $H=1000$  Oe and  $K=0$  are shown vs temperature as the circles in Fig. 2. The measured  $\Delta F$  is not constant, as would be expected in the commonly assumed Arrhenius model of thermally activated processes. What is even more striking is that  $\Delta E$ , the difference in average energy between the bin containing the saddle point and that containing the metastable minimum as calculated by Eq. (1), is always negative. (The absolute value of  $\Delta E$  is of the same order of magnitude as  $\Delta F$ , but generally lies within one standard deviation of zero.) This is consistent with  $E$  vs  $M_z$  shown in the inset of Fig. 2 (along with the contribution from the various terms) for one reversal at  $H=1000$  Oe,  $T=10$  K, and  $K=0$ . The total energy is seen to be nearly constant for  $M_z > 0.80$ , which is the region around the barrier. Since the free energy is the sum of  $E$  and  $-TS$ , where  $S$  is the entropy, it is reasonable to conclude that the dominant contribution to the positive free-energy barrier is a decrease in entropy going from the metastable minimum to the saddle point.

It should be noted that  $\Delta E$  is measured from the total energy averaged in bins of  $M_z$ , and it is possible that the saddle point is associated with extreme values of  $E$  within the bin. In that case, even though  $\Delta E$  measured from the average energy of the bin is negative, it could be possible that the  $\Delta E$  associated with the reversal is positive. However, no support for extreme values of  $E$  is seen in  $E$  vs  $M_z$  or  $E$  vs  $t$  for individual reversals under a variety of conditions.

The effect of a weaker applied field was also investigated. For  $H=900$  Oe and  $K=0$  results are shown in both figures as squares. There is a small decrease in  $M_z$  at the saddle point, and a significant increase in the free-energy barrier. These results are what one normally expects when the field is lowered, and the difference in energies between the metastable and stable magnetizations decreases. Results for  $H=1000$  Oe and an anisotropy energy of  $K=1.9 \times 10^{-13}$  erg are shown in the figures as diamonds. The broken line in Fig. 1 is a best fit, which shows that  $M_z$  at the saddle point is much less temperature dependent, than in the  $K=0$  case. The free-energy barrier is increased by increasing

$K$ . Although the estimates of  $\Delta F$  are more uncertain for  $K=1.9 \times 10^{-13}$  erg (a consequence of decreased sampling due to the higher barrier), and data are available only for  $T \geq 40$  K, the data indicate that the temperature dependence of  $\Delta F$  may be suppressed by nonzero  $K$ . The measured  $\Delta E$  are negative, even for this value of  $K$ .

The reversal process was also simulated with a precession-free kinetic Monte Carlo (MC) method, which corresponds to the overdamped limit of the LLG equation,<sup>10</sup> to estimate the effect of the underdamped precession of the spins. In this dynamic, one spin is selected at random and is tentatively displaced by a step uniformly distributed on a sphere of radius  $R=0.005$ . Using Eq. (1) to calculate the energies, the displacement is accepted or rejected using the Metropolis method. The spins are normalized after each move to conserve their length. Monte Carlo simulations were performed only for  $H=1000$  Oe and  $K=0$ . The  $M_z$  of the saddle point, the triangles in Fig. 1, are larger than those found using the LLG dynamics, but the dependence on temperature appears to be linear. The free-energy barrier is smaller than that measured for the LLG dynamics at high temperature, but the difference decreases as the temperature is decreased. Even for precession-free MC dynamics, all measured  $\Delta E$  are negative.

In summary, details of the magnetization reversal in underdamped, nanoscale magnets have been investigated with Projective Dynamics. The magnetization at the saddle point has been measured and found to decrease linearly with temperature for  $T < 100$  K. In contrast to the Arrhenius model, which assumes a temperature-independent barrier, the measured free-energy difference between the saddle point and the metastable magnetization is found to be temperature dependent. For the physically reasonable parameters considered here, the difference in the average energy between the saddle point and the metastable magnetization is negative, while the difference in the free energy is positive. From this we conclude that the free-energy barrier under these conditions is due to reduced entropy at the saddle point. Although the temperature dependence of the barrier is weaker, Monte Carlo simulations of overdamped dynamics show the same dominance of entropic contributions to the free-energy barrier.

This work was supported by the Laboratory Directed Research and Development Program of Oak Ridge National Laboratory, managed by UT-Battelle, LLC for the U.S. Department of Energy under Contract No. DE-AC05-00OR22725, by the Ames Laboratory, which is operated for the U.S. Department of Energy by Iowa State University under Contract No. W-7405-82, by the National Science Foundation under Grant 0120310, and by Florida State University through CSIT and MARTECH.

- 
- <sup>1</sup> J.J.M. Ruigrok, R. Coehoorn, S.R. Cumpson, and H.W. Kesteren, J. Appl. Phys. **87**, 5398 (2000).  
<sup>2</sup> M. Kolesik, M.A. Novotny, and P.A. Rikvold, Phys. Rev. Lett. **80**, 3384 (1998).  
<sup>3</sup> M.A. Novotny, Int. J. Mod. Phys. C **10**, 1483 (2000); *Annual Reviews of Computational Physics IX*, edited by D. Stauffer (World Scientific, Singapore, 2001), p. 153.  
<sup>4</sup> S.J. Mitchell, M.A. Novotny, and J.D. Muñoz, Int. J. Mod. Phys. C **10**, 1503 (2000).  
<sup>5</sup> S. Wirth, M. Field, D.D. Awschalom, and S. von Molnár, Phys. Rev. B **57**, R14028 (1998); J. Appl. Phys. **85**, 5249 (1999).  
<sup>6</sup> G. Brown, M.A. Novotny, and P.A. Rikvold, Phys. Rev. B **64**, 134422 (2001).  
<sup>7</sup> W.F. Brown, Phys. Rev. **130**, 1677 (1963).  
<sup>8</sup> A. Aharoni, *Introduction to the Theory of Ferromagnetism* (Clarendon, Oxford, 1996).  
<sup>9</sup> G. Brown, M.A. Novotny, and P.A. Rikvold, in *Computer Simulation Studies in Condensed Matter Physics XV*, edited by D.P. Landau, S.P. Lewis, and H.-B. Schüttler (Springer, Berlin, in press).  
<sup>10</sup> U. Nowack, R.W. Chantrell, and E.C. Kennedy, Phys. Rev. Lett. **84**, 163 (2000).

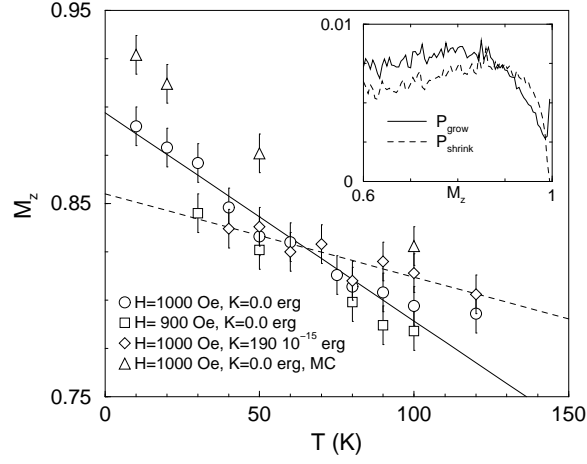


FIG. 1. Saddle-point magnetization along the pillar,  $M_z$ , estimated from  $P_{\text{grow}} = P_{\text{shrink}}$ , shown vs temperature,  $T$ , under different conditions. The solid line is a best fit to the results for  $T \leq 100$  K at  $H=1000$  Oe and  $K=0$ , and the broken line is a best fit for  $H=1000$  Oe and  $K=190 \times 10^{-15}$  erg. The data for a weaker field,  $H=900$  Oe, and over-damped dynamics also change approximately linearly with temperature. The probabilities  $P_{\text{grow}}$  and  $P_{\text{shrink}}$  for  $H=1000$  Oe,  $T=10$  K, and  $K=0$  are shown in the inset. The right-most crossing occurs at the metastable minimum, and the left-most crossing shown occurs at the saddle point.

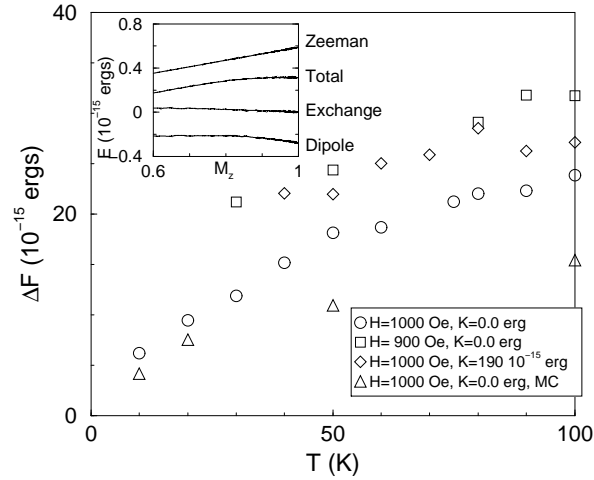


FIG. 2. Free-energy barrier associated with magnetization reversal,  $\Delta F$ , measured from the residence time,  $h$ , shown vs temperature  $T$ . The measured switching times for various conditions varied from 7.5 ns ( $T=90$  K,  $H=1000$  Oe,  $K=0$ ) to 143.2 ns ( $T=10$  K,  $H=1000$  Oe, Monte Carlo). All energy differences,  $\Delta E$ , are negative (not shown). The inset shows the energy, defined in Eq. (1), vs  $M_z$  for one reversal event at  $H=1000$  Oe,  $T=10$  K, and  $K=0$ . The curve is parametric with respect to the simulation time, and it is not single valued near the metastable magnetization.